

Water Release from Pyrophyllite during the Dehydroxylation Process Explored by Quantum Mechanical Simulations

Esther Molina-Montes,[†] Davide Donadio,[‡] Alfonso Hernández-Laguna,[§] Michele Parrinello,[⊥] and C. Ignacio Sainz-Díaz^{*,§}

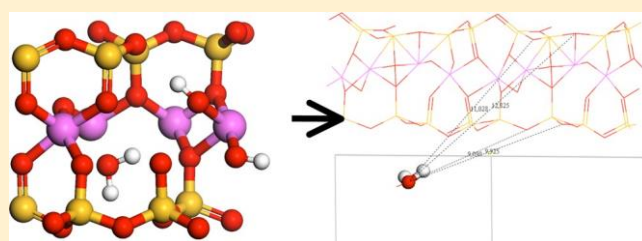
[†]Escuela Andaluza de Salud Pública, Cuesta del Observatorio 4, 18080-Granada, Spain, and Ciber Epidemiología y Salud Pública, CIBERESP, Spain

[‡]Department of Chemistry, University of California at Davis, One Shields Avenue, Davis, California 95616, United States

[§]Instituto Andaluz de Ciencias de la Tierra, CSIC-Universidad de Granada, Avenida de las Palmeras, 4, 18100-Armilla, Granada, Spain

[⊥]ETH-Computational Center Lugano, Switzerland

Abstract: We have investigated one of the most controversial aspects of the dehydroxylation–rehydroxylation process of dioctahedral 2:1 phyllosilicates, that is the release of water from the internal structure of the mineral. We simulate the release of water from a periodic crystal model of pyrophyllite by Car–Parrinello molecular dynamics based on Density Functional Theory. The metadynamics algorithm is employed to accelerate activated processes and compute free energy surfaces. We found that, in spite of the strong hydrogen bonds anchoring water molecules in the tetrahedral cavity, the energy barrier for water release is lower than that for the chemical formation of water molecules from the hydroxyl groups. We then conclude that water release is not the rate-limiting step of the dehydration mechanism.



INTRODUCTION

The thermal stability of clays is associated with their physical-chemical properties. High temperature leads to chemical and structural transformations that may be advantageous for applications in ceramics, refractory materials, and pressure-transfer media, but can also lead to thermal degradation. For this reason, a deeper knowledge of the thermal behavior of clay minerals is needed.

Dehydroxylation of pyrophyllite, a dioctahedral 2:1 phyllosilicate, in which a sheet of octahedrally coordinated Al cations is sandwiched between two sheets of linked silica tetrahedra, comprises three well-established steps: First, a reaction of two neighboring hydroxyl groups resulting in the formation of a H₂O molecule; second, this water molecule diffuses through the octahedral vacancy to the tetrahedral cavity; and finally water migrates to the interlaminar region, from which it can diffuse out of the structure. Several aspects of this process have been studied exhaustively in many experimental studies which have given insight to the following facts: Structural changes take place mainly in the octahedral sheet, while the tetrahedral sheet remains undistorted at the end of this process. In particular, the final dehydroxylated structure consists of five-coordinated Al cations linked by a residual bridging oxygen, which is the one that previously donated a proton.^{1,2} The reaction occurs over a broad

as a combination of processes of dehydroxylation–rehydroxylation.⁴

Regarding kinetics, the migration of the water molecule throughout the tetrahedral cavity has been proposed as the rate-limiting step of this reaction in some studies.⁵ Controversies still remain in relation to the mechanism⁶ and the activation energy required for each step, and for the entire dehydroxylation reaction.^{7,8} The low crystallinity, the high degree of disorder, and the high dispersion in particle size make the correct interpretation of the experiments difficult. Since many aspects of the mechanism and structural transformations are still poorly understood, theoretical modeling can provide major contributions.

Quantum mechanical calculations have been used to study the dehydroxylation reaction in order to achieve an understanding of this process at the atomic scale. From these calculations, the energetics of the dehydroxylation reaction was accurately determined, finding that dehydroxylation goes throughout three possible mechanisms: (i) the on-site mechanism involving the bridging hydroxyl groups of an octahedral cation pair; (ii) the cross mechanism where two hydroxyl groups react across the octahedral vacancy; and (iii) involving the assistance of the apical oxygens.⁹ The first step of the reaction can generate intermediates: the cross and on-site semidehydroxylate states.^{9,10}

range of temperatures from 350 to 850 °C, and it is reversible as the initial structure of pyrophyllite can be recovered when the critical temperature of amorphization has not been reached.³ The dehydroxylation reaction has been considered by some authors

According to our previous calculations, the intermediate structures are strongly metastable, hindering complete and spontaneous dehydroxylation. Furthermore, rehydroxylation turned out to be competitive with the dehydroxylation process.¹¹ Therefore, it is plausible that more energy is required for further progress of this reaction.

Here we aim to investigate the *final* step of the dehydroxylation reaction, that is the migration of the water molecule out of the structure, by starting from the semidehydroxylate derivatives. Our results suggest that the migration of water is thermodynamically favored requiring a lower energy barrier than the dehydroxylation–rehydroxylation step.

METHODS

Car–Parrinello molecular dynamics (MD)¹² based on the Density Functional Theory (DFT) has proven to be a useful tool for exploring complex processes in the solid state.¹³ We used herein the CPMD package v.3.9¹⁴ within the generalized gradient approximation (GGA) with the BLYP parametrization for the exchange–correlation functional^{15,16} along with Troullier–Martins norm-conserving pseudopotentials,¹⁷ and a energy cutoff of 70 Ry. In our system water molecules interact with the mineral mostly via hydrogen bonds. Given the fast development of dispersion methods within DFT and the lack of a general assessment on their beneficial effects,¹⁸ we decided to rely upon standard GGA functionals, for which performances and limitations are well established. Simulations were performed at constant volume and constant temperature within a complete unit cell including the interlayer space. In our system, a periodic crystal model of pyrophyllite taken from crystallographic data,⁶ a standard MD run was shown to require an unfeasibly long simulation time to explore the complex process of dehydroxylation in the solid state. However, the metadynamics method allows an *efficient* study of complex processes in condensed phases, and an estimation of the free energy profile.^{19,20} The metadynamics approach has previously proven to be *efficient* for exploring the dehydroxylation reaction.²¹

Metadynamics is based on the definition of collective variables (CV), which are analytic functions of the relative atomic positions, and define a coarse-grained space to explore the reaction path. The functional form and the details of the use of these CVs are reported elsewhere.^{22,23} Interatomic distances (D)

were used as collective variables to explore this last step of the

reaction. They were defined between the O atom of the water molecule and an O atom of the tetrahedral sheet, i.e., one D (D1) for the distance between the water molecule oxygen and one O atom of the upper tetrahedral sheet, and a second D (D2) for the distance between the water molecule oxygen and one O atom of the lower tetrahedral sheet. The dynamics in the space of the CVs is coupled to the dynamics of the real system and is biased by a history-dependent potential made of Gaussians with a suitable width and height, centered on the trajectory of the CVs. The biasing potential helps to overcome the local minima of the free energy surface (FES), forcing the system to explore the relevant parts of the coarse grained space defined by the CVs. The sum of the Gaussians provides an estimation of the FES with an accuracy that depends on the dimensionality of the CV space, their diffusion coefficient, and the parameters of the history-dependent potential. The widths of the Gaussians for CVs were set to 0.01–0.02 Å at 900 K, and to 0.02–0.03 Å at 1500 K, being $1/5$ of the amplitude of the CV fluctuations at the equilibrium. Spherical Gaussian hills with a fixed height of 1.25

kcal/mol were added approximately every 10 fs. The height is much smaller than the potential energy barriers estimated for the dehydroxylation reaction of previous works, both theoretically²⁴ and experimentally.²⁵ Finally, the parameters of the Gaussians that form the history-dependent potential have been chosen, so to reproduce the free energy surface with an accuracy of ~ 2 kcal/mol.

When the reaction trajectories from metadynamics were identified, we explored the topology of the Free Energy Surface (FES), where we identified the critical points (minima and transition states) and characterized them by means of quantum mechanical calculations at 0 K. The transition states were optimized by the PRFO algorithm²⁶ and also confirmed by computing the negative eigenvalues of the Hessian matrix along the reaction coordinate

RESULTS AND DISCUSSION

With a periodic model of crystal lattice structure of pyrophyllite, we can explore two possible mechanisms of dehydroxylation, on-site and cross, which have been previously reported.^{9,21} We found the reaction path and transition states of both mechanisms, both having a similar activation energy at 0 K for the formation of the semidehydroxylate intermediate (59.7 and 58.8 kcal/mol for on-site and cross mechanisms, respectively). These values are consistent with previous cluster model calculations²⁷ and with experimental values.²⁴ However, taking into account finite temperature effects by molecular dynamics simulations, and computing the free energy surface of the reaction, we observed that the activation free energy of the cross mechanism (38 and 37 kcal/mol at 900 and 1500 K, respectively) is lower than the on-site one (50 and 46 kcal/mol at 900 and 1500 K, respectively).⁹

Additional possible mechanisms were found following the on-site and cross ways implying the participation of the apical oxygen atoms, which may form silanol groups. This confirmed the observation of the formation of silanol groups during the dehydroxylation of phyllosilicates by Kloprogge et al.,²⁸ though they proposed the silanol groups of the crystal edges, whereas we found that the H atom of the octahedral OH group is transferred to the apical surrounding SiO group of the crystal lattice where the reaction happens and not only in the edges. Nevertheless, the activation energy of this mechanism was higher than that of the direct paths and the mechanism is more complex. The difference is such that complex dehydroxylation paths involving apical

oxygen atoms should also be considered to occur in the

experiments.¹¹

The semidehydroxylate derivative without the water molecule of the above first step can be completely dehydroxylated throughout the on-site mechanism, showing a similar activation energy (60 kcal/mol), but showing a lower free energy barrier (31 and 29 kcal/mol at 900 and 1500 K) than the first step. On the other hand, the cross mechanism of this second reaction step (the formation of the second water molecule per unit cell) is more favorable with a lower free energy (21 and 11 kcal/mol at 900 and 1500 K). However, in all these simulations of the dehydroxylation process, the water molecule remains trapped in the tetrahedral cavity in the final dehydroxylate product, and several side reactions can occur.¹¹ The water molecule, before being released from the tetrahedral cavity, can react with the octahedral cations yielding a rehydroxylation reaction and forming the semidehydroxylated intermediate state with low activation free energy (11 and 13 kcal/mol for cross and on-site mechanisms at 900 K, respectively) and reversible reconversions between the on-site and cross semidehydroxylate intermediates

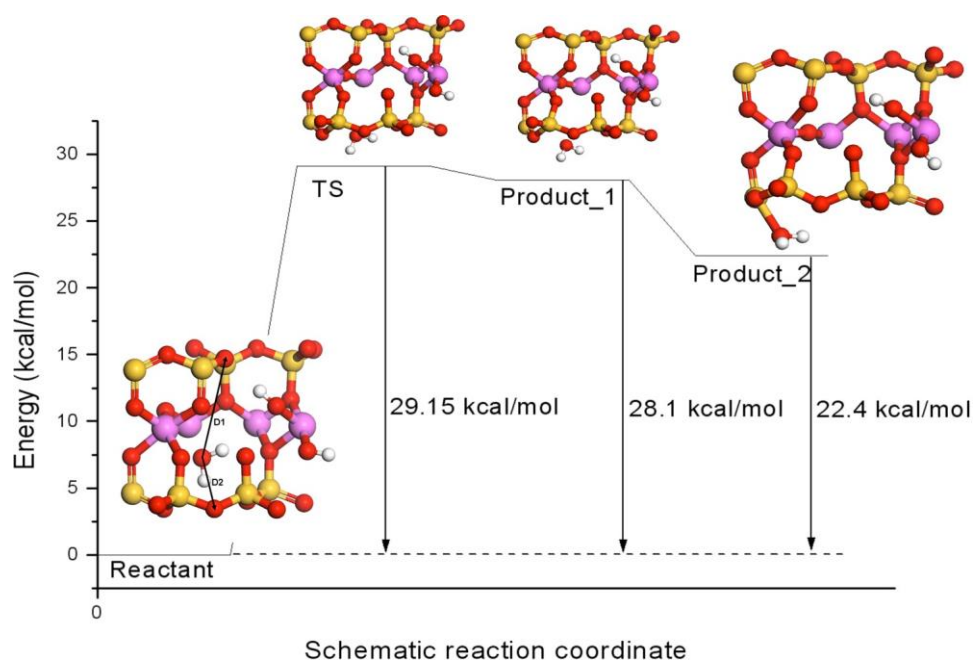


Figure 1. Critical points optimized at 0 K of the reaction path for the water migration from the semidehydroxylate intermediate (the CV's as described in the figure) of the on-site mechanism of dehydroxylation. The H, O, Al, and Si atoms are in white, red, pink, and yellow, respectively.

can also occur. Besides, this rehydroxylation reaction can be facilitated by the participation of apical tetrahedral oxygens, forming silanol groups and decreasing the activation free energy in the cross mechanism to 3.5 and 1.5 kcal/mol at 900 and 1500

K, respectively.²⁷ Furthermore, the rehydroxylation reaction

requires less energy than the dehydroxylation while the water molecule remains inside the tetrahedral cavity, and hence, this water should migrate to the interlayer space for a complete evolution of the dehydroxylation reaction.

To explore this reaction further, we investigate the migration of water from the tetrahedral cavity to the interlayer space in a crystal lattice model using MD and metadynamics simulations. Two CV's were chosen: D1, the distance of the O atom of water molecule trapped inside the tetrahedral cavity with any basal O atom of the tetrahedral cavity; and D2, the distance of the water O atom inside the tetrahedral cavity with one basal O atom of the other tetrahedral sheet (Figure 1).

Starting with the semidehydroxylate derivative of the on-site mechanism (Figure 1), the water molecule is initially inside the tetrahedral cavity, and has to migrate through the cavity to go out to the interlayer space. Following the evolution of the CV's, D1 and D2, during the MD simulations of the water migration process, we can observe at 900 K a drastic change of D2 to larger values (Figure 2a), indicating the migration of the water molecule from the initial position to the interlayer and to the vicinal unit cell. Similar behavior was observed at 1500 K. Observing the free energy profile with respect to the CV's at 1500 K (Figure 2b), the minimal energy structure of reactant is localized within a broad low energy zone where both CV's fluctuate with the thermal energy due to the movement of the water molecule around the tetrahedral cavity. A reaction path is localized during the formation of the intermediates as minimum energy points (blue spots at high values of D1 and D2) with a saddle point between these intermediates and reactants. The high

was estimated as 24.2 and 13.8 kcal/mol at 900 and 1500 K, respectively.

From these trajectories, the critical points of this reaction path

were optimized at 0 K, finding an activation energy of 29.1 kcal/mol (Figure 1).

The migration of water through the tetrahedral cavity yields two intermediates: one (product 1), 28.1 kcal/mol less stable than the semidehydroxylate derivative of pyrophyllite, with the water molecule close to the basal oxygens of the surface of tetrahedral cavity; and the other one (product 2), 5.7 kcal/mol more stable than the latter one, where the water molecule comes from the vicinal cell and is close to one edge and out of the tetrahedral surface. No additional TS was found in this section of the FES. Nevertheless, the transition between these intermediates will pass through one TS with low energy in this FES region. Considering the reverse reaction way, the energy barrier is very low, 6.75 kcal/mol from product 2. This means that the presence of water on the product surface will provoke almost spontaneously the penetration of water inside the tetrahedral cavity. In the last step, the water molecule diffuses along the interlayer space, however, no critical points were detected due to the flatness of the potential energy surface.

The release of water from the semidehydroxylate intermediate in the cross mechanism of dehydroxylation was explored with the same CV set. From the free energy profile with respect to CV's, we estimate an activation free energy of 18.7 kcal/mol at 900 K, close to that estimated for the on-site mechanism (Figure 3a). Along the free energy surface we can localize the reactant, as a minimum with low values of CV's, and the product, as a minimum surrounded by secondary minima at large values of CV's, finding a saddle point between them. This product can be considered as an intermediate with the water molecule on the surface of the tetrahedral cavity. Then, the last step of water diffusion along the interlayer space has an activation free energy

of 9.2 kcal/mol at 900 K.

Considering the completely dehydroxylated intermediate with the water molecule inside the tetrahedral cavity, we explored the release of water with the same CV set. Observing the profile of values of D1 and D2 are higher than if the water molecule were in the interlayer space of the same unit cell and hence the water molecule will diffuse to the next vicinal unit cell (Figure 2c). From these free energy profiles the activation free energy

Draft

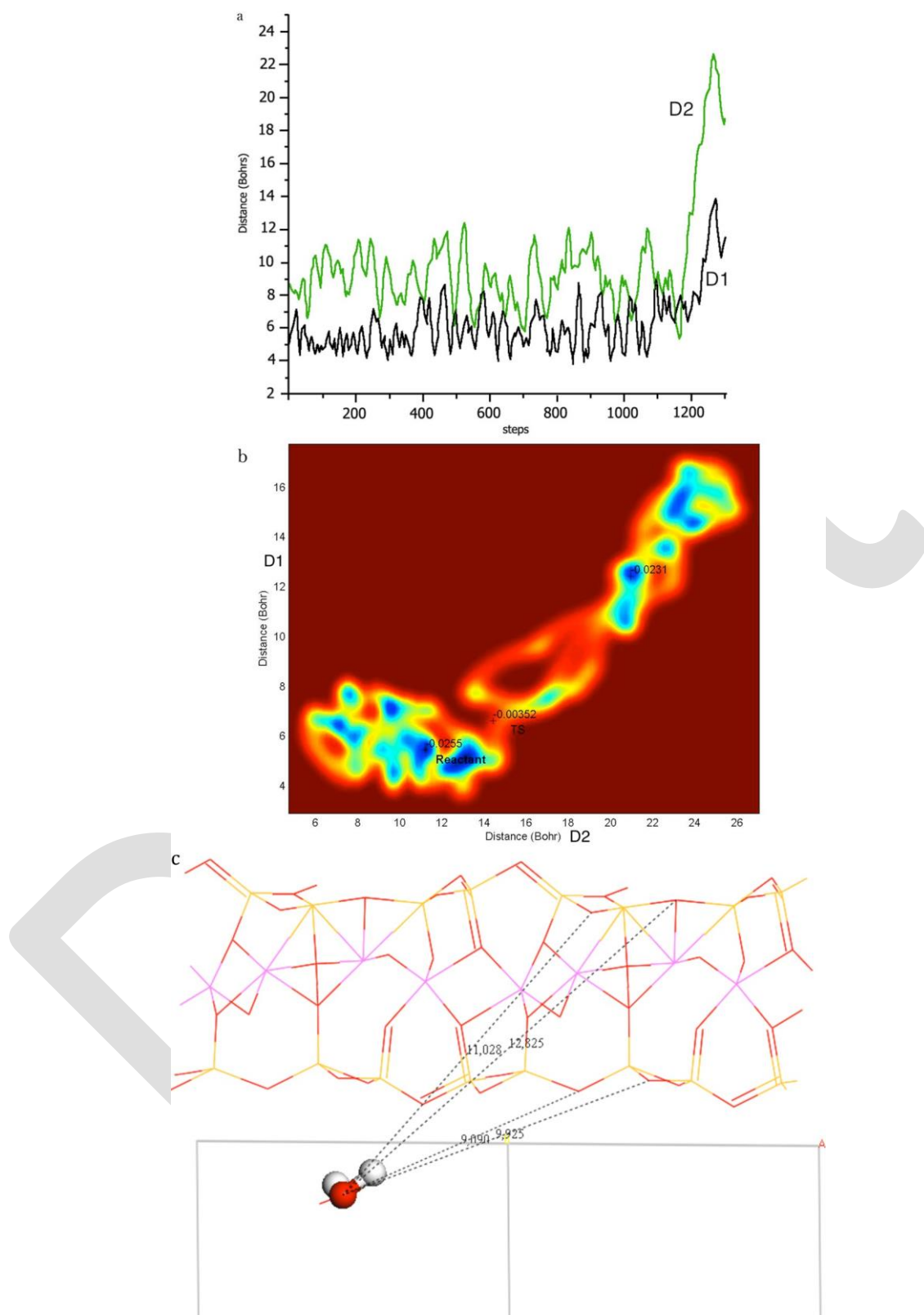


Figure 2. (a) Evolution of the CV's along the MD simulations of the water migration at 900 K (D1 and D2 are in black and green, respectively). (b) Free energy surface with respect to CV of the migration of water from the semidehydroxylate intermediate of the on-site mechanism at 1500 K. The free energy (hartrees) is plotted against the CV's (D1 in the y-axis and D2 in the x-axis) by means of isoenergetic curves with a color profile from blue (lowest energy) until dark red (highest value). (c) Snapshot of the simulation at 1500 K highlighting the water molecule formed in the unit cell of the right part and diffusing to the vicinal unit cell on the left.

the free energy surface with respect to CV's at 900 K, the reactant can be detected as a minimum (blue zone) with both CV values

close to 9–10 bohrs and other minima are found at higher values of CV corresponding to the products (Figure 3b). The water

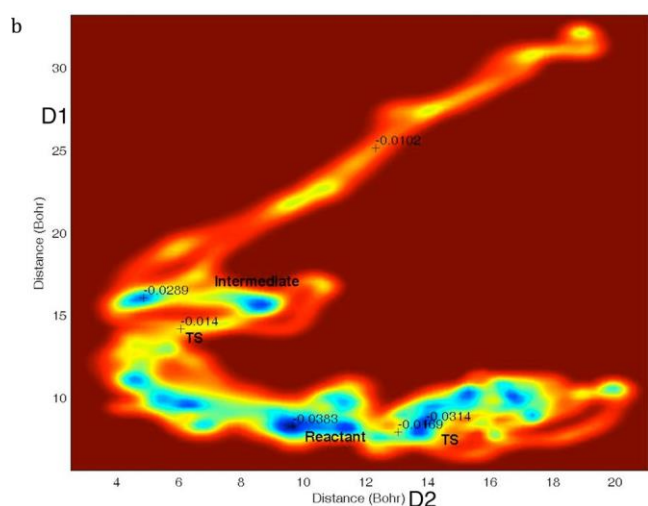
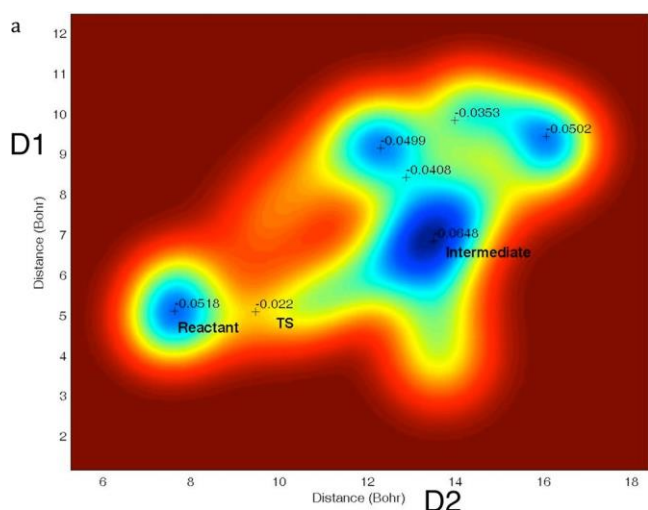


Figure 4. The migration of water from the dehydroxylate intermediate with water inside the tetrahedral cavity (b) at 900 K. The free energy (hartrees) is plotted against the CV's (D1 in the y-axis and D2 in the x-axis) by means of isoenergetic curves with a color profile from blue (lowest energy) until dark red (highest value).

molecule tries to escape downward and upward (along the [001] direction) from the octahedral vacancy site toward the up and down tetrahedral cavities exploring several trajectories. Initially this molecule goes toward the external surface of the tetrahedral cavity where it is trapped, at larger value of D2 and close to the initial value of D1. However, this intermediate is not stable and after further simulation steps the water molecule goes back to the initial position and goes out through the other tetrahedral cavity decreasing drastically D2 and increasing D1, forming an intermediate with the water molecule over the external surface of this tetrahedral cavity (the opposite one to that where initially this molecule was trapped). Eventually the water molecule diffuses away increasing both CV's, D1 and D2. Similar behavior was detected at 1500 K. From this FES we can estimate an approximate activation free energy of 15.2 and 15.5 kcal/mol at 900 and 1500 K, respectively. The final step is the diffusion of water molecule along the interlayer space with an activation free

energy of 11.7 kcal/mol, similar to that in the cross-semidehydroxylate derivative (9.2 kcal/mol).

In general, the energy barrier of the migration of water is lower than that of the initial formation of water. Our calculations show that the final product (a completely dehydroxylated product plus two released water molecules) is 24.9 kcal/mol less stable than pyrophyllite, being consistent with previous DFT calculations (28.5 kcal/mol).⁹ Taking into account the activation free energy of our simulations, this free energy is lower in the water migration and water diffusion than in the formation of water molecule during the dehydroxylation process (Table 1). The free energy

Table 1. Activation Free Energies (kcal/mol) Estimated from the Different Steps of the Dehydroxylation Process

	900 K	1500 K
on-site mechanism		
water formation from pyrophyllite	49.9	45.8
water formation from semidehydroxylate ^o	30.9	29.0
rehydroxylation	13.1	7.4
interconversion—rehydroxylation of intermediates (from on-site to cross) ^o	34.1	
water migration from the first step intermediate (semidehydroxylate-on-site + water)	24.2	13.8
water migration from the final intermediate (dehydroxylate + water) ^o	15.2	15.5
water diffusion over the completely dehydroxylated product	11.7	
cross mechanism		
water formation from pyrophyllite	48.3	38.7
water formation from semidehydroxylate ^o	21.2	11.3
rehydroxylation	3.5	1.5
interconversion of intermediates (from cross to on-site) ^o	20.2	11.0
water migration from the first step intermediate (semidehydroxylate-cross + water)	18.7	
water diffusion over semidehydroxylate-cross	9.	

barriers for water migration are similar for both on-site and cross mechanisms, being slightly lower in the cross path. In the last stage of the complete dehydroxylation process (Figure 4), the water migration of the dehydroxylate product has a free energy barrier slightly lower than in the previous semidehydroxylate intermediates.

CONCLUSIONS

The first principles molecular dynamics simulations yield a good estimate of the activation free energy of the main steps of the whole dehydroxylation reaction. In all cases, the migration of water through the tetrahedral cavity and the diffusion of water through interlayer space have a lower energy barrier than the formation of water. Therefore, the initial step of water formation is the limiting step of the whole dehydroxylation reaction of pyrophyllite. This contrasts with the interpretations of Gualtieri and Ferrari⁵ based on experimental kinetic studies that concluded that the limiting step was the migration of water. After the water formation step many processes can occur: the highly favored rehydroxylation, interconversion between intermediates, water migration from the tetrahedral cavity to the interlayer surface, and water diffusion over the surface. Hence, all these fast processes can change the real kinetic equation model even when these intermediates cannot be detected.

Within the equilibrium in the water—mineral system, the evaporation of water makes a shift of the equilibrium toward the

formation of the dehydroxylate derivatives avoiding the rehydroxylation and the intermediates exchange. A further

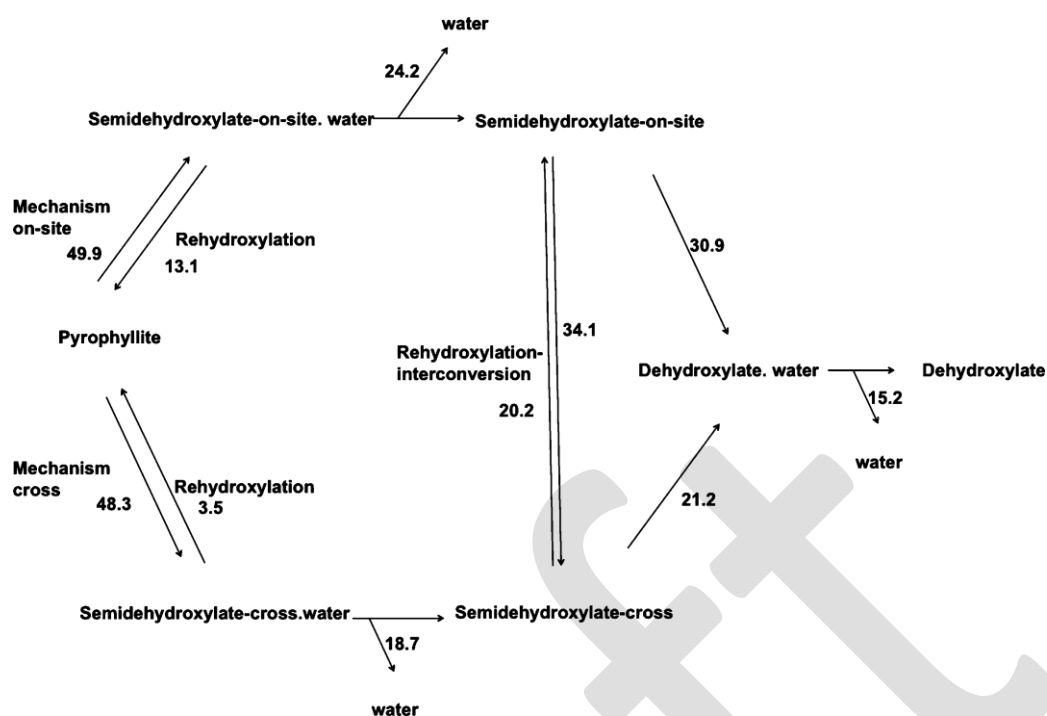


Figure 4. Scheme of the complete dehydroxylation process of pyrophyllite including the steps and intermediates. Activation free energy values at 900 K (in kcal/mol) are included.

expose of moisture on the dehydroxylate derivatives will yield the rehydroxylation even at high temperatures. Hence the water migration has lower activation free energy than the water formation, however, the release of water is very important for a complete evolution of the process. The kinetics of water release affects the formation of all these intermediates. Besides, the migration and diffusion of water is highly dependent on the crystal size, and the smaller the crystal the faster the release of water, and the shorter the average life of the intermediates. This conclusion is consistent with previous experimental interpretations of the high dependence of particle size to the kinetics of the whole dehydroxylation process.⁷

ACKNOWLEDGMENTS

Authors are thankful to the Centro Técnico de Informática de CSIC, centro de Cálculo del CIEMAT, Centro de Cálculo de Galicia (CESGA), and the Centro de Supercomputación de la Universidad de Granada (UGRGRID) for allowing the use of its computational facilities; to Computational Centre of ETH in Lugano for its support; and Daniella Witz for her help. This work was supported by the Spanish MCYT and European FEDER grants CGL2005-02681, CGL2008-02850, and CGL2008-06245-CO2-01, and CSIC through the I3P program, and the Junta de Andalucía grant for the RNM363 PAIDI group.

REFERENCES

- (1) Fitzgerald, J. J.; Dec, S. F.; Hamza, A. I. *Am. Mineral.* 1989, *74*, 1405.
- (2) Frost, R. L.; Barron, P. F. *J. Phys. Chem.* 1984, *88*, 6206.

- (3) Derkowski, A.; Drits, V. A.; McCarty, D. K. *Am. Mineral.* 2012, *97*, 610.
- (4) Heller, L.; Farmer, V. C.; Mackenzie, R. C.; Mitchell, B. D.; Taylor, H. F. W. *Clay Miner. Bull.* 1962, *5*, 56.
- (5) Gualtieri, A. F.; Ferrari, S. *Phys. Chem. Miner.* 2006, *33*, 490.
- (6) Guggenheim, S.; Chang, Y. H.; Van Groos, A. F. K. *Am. Mineral.* 1987, *72*, 537.
- (7) Drits, V. A.; Derkowski, A.; McCarty, D. K. *Am. Mineral.* 2011, *96*, 153.
- (8) Drits, V. A.; Derkowski, A.; McCarty, D. K. *Am. Mineral.* 2012, *97*, 930.
- (9) Molina-Montes, M. E.; Donadio, D.; Sainz-Díaz, C. I.; Hernández-Laguna, A.; Parrinello, M. *J. Phys. Chem. B* 2008, *112*, 7051.
- (10) Sainz-Díaz, C. I.; Escamilla-Roa, E.; Hernández-Laguna, A. *Am. Mineral.* 2004, *89*, 1092.
- (11) Molina-Montes, E.; Donadio, D.; Hernandez-Laguna, A.; Sainz-Díaz, C. I. *J. Phys. Chem. B* 2010, *114*, 7593.
- (12) Car, R.; Parrinello, M. *Phys. Rev. Lett.* 1985, *55*, 2471.
- (13) Churakov, S. V.; Iannuzzi, M.; Parrinello, M. *J. Phys. Chem. B* 2004, *108*, 11567.
- (14) CPMD, version 3.9.2., IBM Corp., MPI fuer Festkoerperforschung Stuttgart: Stuttgart, Germany, 2004.
- (15) Becke, A. D. *Phys. Rev. [Sect.] A* 1998, *38*, 3098.
- (16) Lee, C.; Yang, W.; Parr, G. M. *Phys. Rev. [Sect.] B* 1988, *37*, 785.
- (17) Troullier, N.; Martins, J. L. *Phys. Rev. [Sect.] B* 1991, *43*, 1993.
- (18) Liu, Y.; Zhao, J.; Li, F.; Chen, Z. *J. Comput. Chem.* 2013, *34*, 121.
- (19) Laio, A.; Parrinello, M. *Proc. Natl. Acad. Sci. U.S.A.* 2002, *99*, 12562.
- (20) Laio, A.; Rodríguez-Forteza, A.; Gervasio, F.; Ceccarelli, M.; Parrinello, M. *J. Phys. Chem. B* 2005, *109*, 6676.
- (21) Molina-Montes, M. E.; Donadio, D.; Hernández-Laguna, A.; Sainz-Díaz, C. I. *J. Phys. Chem. A* 2008, *112*, 6373.
- (22) Iannuzzi, M.; Laio, A.; Parrinello, M. *Phys. Rev. Lett.* 2003, *90*, 238.
- (23) Laio, A.; Gervasio, F. L. *Rep. Prog. Phys.* 2008, *71*, 126601.
- (24) Stackhouse, S.; Coveney, P. V.; Benoit, D. M. *J. Phys. Chem. B* 2004, *108*, 9685.
- (25) Bray, H. J.; Redfern, S. A. T. *Mineral. Mag.* 2000, *64*, 337.
- (26) Billeter, S. R.; Curioni, A.; Andreoni, W. *Comput. Mater. Sci.* 2003, *27*, 437.

(27) Molina-Montes, E.; Timón V.; Hernández-Laguna, A.; Sainz-Díaz, C. I. *Geochim. Cosmochim. Acta* 2008, 72, 3929.

(28) Klopogge, J. T.; Kamarneni, S.; Yanagirawa, K.; Fry, R.; Frost, R. L. J. *Colloid Interface Sci.* 1999, 212, 562.

Draft